

# Experimental investigation of carbon dioxide hydrate formation in a colloidal solution of H<sub>2</sub>O+ SDS + SiO<sub>2</sub> at a constant SiO<sub>2</sub> concentration of 300 ppm

Elizaveta Shemeleva<sup>1\*</sup>, Anton Osipov<sup>1</sup>, and Bogdan Klimov<sup>1</sup>

<sup>1</sup>Novosibirsk State University, Novosibirsk, Russia

**Abstract.** The paper presents a experimental investigation of carbon dioxide hydrate formation in a colloidal solution of H<sub>2</sub>O+ SDS + SiO<sub>2</sub>. The influence of the kinetic promoter of sodium dodecyl sulfate (SDS) on the formation of carbon dioxide gas hydrate at various concentrations: 0, 100, 300, 500 ppm was assessed. The SiO<sub>2</sub> concentration in the solution was constant and equal to 300 ppm. The change in solution temperature and pressure during the production of hydrate is shown for each SDS concentration. The values of convection of solution and gas into the gas hydrate state were determined.

## 1 Introduction

Gas hydrates are crystalline solids in which water molecules form a three-dimensional framework of cavities into which gas molecules are incorporated by van der Waals forces. The formation of these compounds occurs under special thermodynamic conditions requiring low temperatures and high pressure.

Gas hydrates have many useful properties, including the ability to concentrate large volumes of gas (up to 170 volumes in one volume of gas hydrate), provide unique conditions of stability at various temperatures and pressures, when violated, they decompose into water and gas. Because of these characteristics, researchers are interested in using gas hydrates in a variety of applications, including natural gas transportation, water desalination, gas storage, cold storage and other purposes. Pilot projects are currently underway to use gas hydrates to transport natural gas. Technological processes using hydrate formation can be used to solve environmental problems associated with carbon dioxide emissions into the atmosphere. There are two main methods for capturing carbon dioxide from gas mixtures: before and after fuel combustion. Pre-combustion capture involves removing CO<sub>2</sub> from synthesis gas, a partially burned fuel containing about 40% CO<sub>2</sub> and 60% H<sub>2</sub>. This method can be more efficient due to the high CO<sub>2</sub> content of the synthesis gas, but requires specific equipment. Post-combustion recovery is less efficient but can be implemented in any plant with minimal modifications.

---

\* Corresponding author: [e.shshemeleva@g.nsu.ru](mailto:e.shshemeleva@g.nsu.ru)

There are various methods for extracting certain gases from gas mixtures such as absorption, adsorption and membrane methods. However, they are all quite energy-intensive, which encourages the search for less energy-intensive alternatives. A recent approach to separating CO<sub>2</sub> from flue gases or CO<sub>2</sub>-H<sub>2</sub> mixtures involves the use of gas hydrate formation [1].

However, despite the breadth of prospects for the use of technologies based on gas hydrates, there is currently no full-fledged industrial implementation of this process due to the complexity of their production. There are many works aimed at both studying the thermodynamic conditions of production [2-5], and the features of their formation [6-9], decomposition and combustion when using various kinetic and thermobaric promoters in water [10-21].

This article discusses the use of physical and chemical promoters, such as porous SiO<sub>2</sub> nanopowder and SDS kinetic promoter, to improve the efficiency of gas hydrate formation.

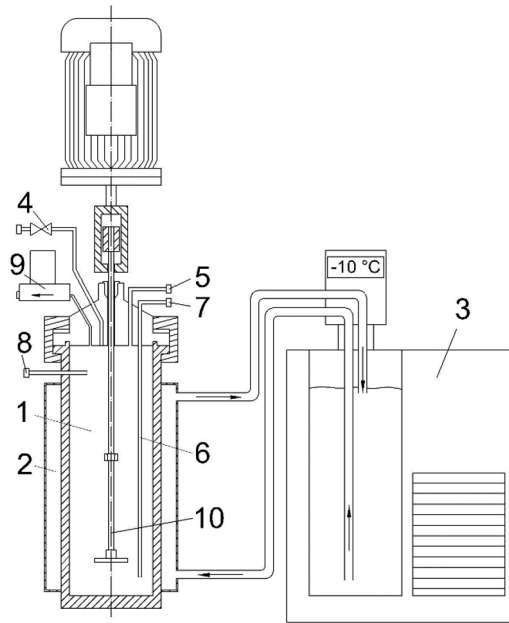
## 2 Experimental setup and method

The experiments were carried out on an autoclave-type installation, which is a cylindrical vessel made of stainless steel with a diameter of 100 mm and a height of 300 mm Figure 1, equipped with two pairs of viewing windows in height. The working area was mixed using a magnetic coupling and a three-bladed stirrer shaft with continuously variable speed control up to 1480 rpm. Cooling was carried out through a liquid jacket located on the outer surface of the vessel by passing coolant from a LOIP FT-316-40 cryothermostat through it. The outer wall of the autoclave was thermally insulated with foam rubber. A Pt-100 temperature sensor was placed through a metal sleeve from the top of the unit to the stirrer level in the working volume. In addition, to work with carbon dioxide, the installation was modified by introducing an OVEN PD-100 pressure sensor with a measured pressure range of 0..10 MPa into the lid.

The colloidal solution was prepared from bidistilled and deionized water, SiO<sub>2</sub> nanoparticles and sodium dodecyl sulfate (SDS). SiO<sub>2</sub> nanoparticles provided by Bardakhanov LLC had a specific surface area of 136 m<sup>2</sup>/g and an average particle size of 20 nm. The solution was prepared using a two-stage method: first, the required amount of SiO<sub>2</sub> nanoparticles and SDS was added to water, then the mixture was intensively stirred. After this, the mixture was processed in an ultrasonic bath Sonorex Super RK 100H at a frequency of 35 kHz and a power of 80 W for an hour at 70 °C. The nanoparticles used were hydrophilic, ensuring the stability of aqueous suspensions. Four samples were prepared with different SDS concentrations (0–500 ppm) and a constant SiO<sub>2</sub> concentration of 300 ppm.

Cooling of the working area of the autoclave was carried out by pumping a coolant with a temperature of -1 °C through a water jacket. A colloidal solution weighing 300 g was placed in the autoclave; his temperature began to drop. At this time, several iterations of purging the system with carbon dioxide were carried out to remove air from the working section. When the solution temperature reached 4 °C, carbon dioxide was supplied from the cylinder into the volume of the autoclave until a pressure of 3 MPa was reached. Next, carbon dioxide dissolved and the pressure decreased by several atmospheres. After the pressure drop stopped and, accordingly, the process of dissolving carbon dioxide in water stopped, carbon dioxide was again supplied to the working area until the pressure in the system reached 3 MPa. After this, mixing of the colloidal solution and the carbon dioxide system was turned on at a frequency of 450 rpm. As a result, the temperature in the working area increased as a result of heat release during the formation of gas hydrates. The nature of hydrate growth and, accordingly, the temperature for all experiments performed are original. At the same time, the pressure constantly decreases, since carbon dioxide, upon

contact with water, transforms into a gas hydrate state. Using the equation of state of carbon dioxide, the mass of carbon dioxide converted into hydrate and then the mass of solution conversion were calculated from the pressure drop.



*1 – working volume of the installation; 2 – cooling jacket; 3 - cryostat; 4 - inlet valve; 5 – pressure sensor; 6 – sleeve for temperature sensor; 7, 8 – temperature sensors, 9 – flow controller; 10 – stirrer [22]*

**Fig. 1.** Scheme of the experimental setup.

### 3 Results and Discussion

A study was carried out on the formation of carbon dioxide hydrate in a colloidal solution of water + SDS + SiO<sub>2</sub> at a constant SiO<sub>2</sub> concentration of 300 ppm and a varying SDS concentration of 0, 100, 300 and 500 ppm. On Figure 2 shows the change in pressure in the system over time. We see a sharp drop in pressure immediately after turning on the stirrer, associated with the dissolution of gas in the solution. And then, after some time, there is a slight drop again, associated with the formation of carbon dioxide gas hydrate. Figure 3 shows the same process, but for changing temperature. Over the course of several minutes, the temperature changes slightly due to the dissolution of carbon dioxide. A second, larger increase in temperature then occurs over a longer period of time, caused by the heat released during hydrate formation.

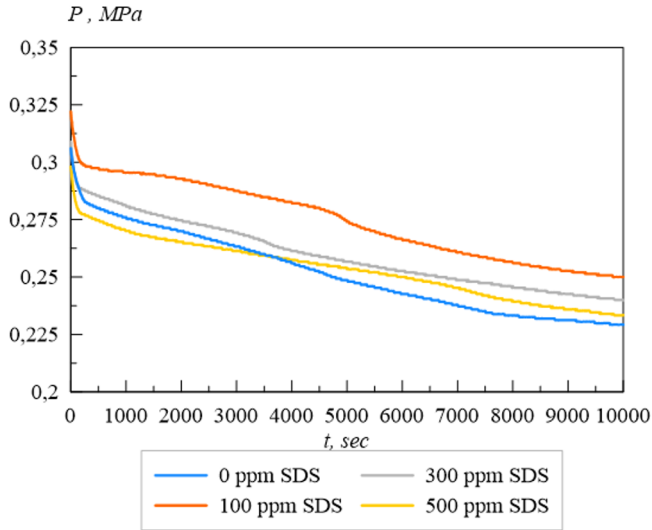


**Fig. 2.** Pressure changes in the system during the for SDS concentrations.

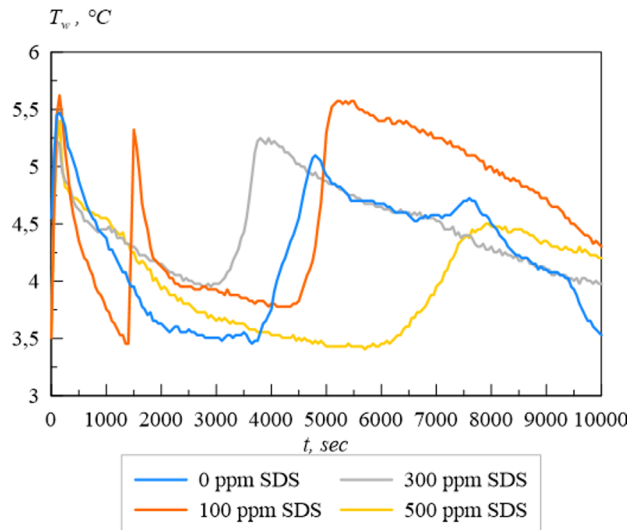


**Fig. 3.** Temperature change in the system during the for SDS concentrations.

Judging by the experimental data obtained for a  $\text{SiO}_2$  concentration of 300 ppm, SDS has a parasitic effect on hydrate formation. At low concentrations of SDS, the inhibition effect is weak, but a further increase in concentration leads to a significant deterioration in the conversion of solution and gas into gas hydrate. At the same time, for 500 ppm  $\text{CO}_2$  the result is expected, due to the formation of reverse micelles on the surface of the  $\text{SiO}_2$  nanoparticle, and for the remaining concentrations obtained, additional research is required. Table 1 shows data on the transition of a colloidal solution to the gas hydrate state at different SDS concentrations and a constant  $\text{SiO}_2$  concentration of 0.3%. Figures 4 and 5 show how the SDS concentration affects the transition of gas and water to the hydrate state relative to the initial amount. The best result was achieved without adding SDS to the solution, at which the conversion of the colloidal solution into water was 28.2%, and into gas - 21%.

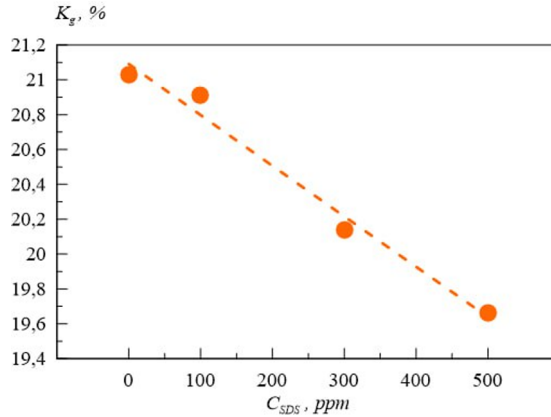


**Fig. 4.** Gas conversion in hydrate for various SDS concentrations: 0, 100, 300, 500 ppm.

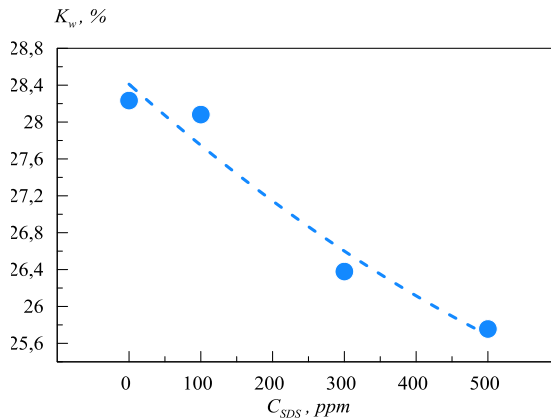


**Fig. 5.** Water conversion in hydrate for various SDS concentrations: 0, 100, 300, 500 ppm.

**Table 1.** Colloidal solution conversion to hydrate state at various SDS concentrations.

<b>Csds, ppm</b>	<b>0</b>	<b>100</b>	<b>300</b>	<b>500</b>
Kg, %	21.0	20.9	20.1	19.7
Kw, %	28.2	28.1	26.4	25.8

## 4 Conclusions

The paper presents the result of experimental studies of the formation of carbon dioxide hydrate in a colloidal solution obtained from water + SiO<sub>2</sub> + SDS with varying SDS concentration 0 – 500 ppm at a constant SiO<sub>2</sub> concentration of 300 ppm. It has been shown that at low concentrations of SDS the inhibition effect is weak, but a further increase in concentration leads to a significant deterioration in the conversion of solution and gas into gas hydrate. At the same time, for 500 ppm CO<sub>2</sub> the result is expected, due to the formation of reverse micelles on the surface of the SiO<sub>2</sub> nanoparticle, and for the remaining concentrations obtained, additional research is required. The best result was achieved without adding SDS to the solution, at which the conversion of the colloidal solution into water was 28.2%, and into gas - 21%.

## Acknowledgements

The work was supported by the Russian Science Foundation (grant no. 22-19-00428).

Link to information about the project: <https://rscf.ru/project/22-19-00428/>

## References

1. S. Skiba, D. Chashchin, A. Semenov, M. Yarakhmedov, V. Vinokurov, A. Sagidullin, A. Manakov, A. Stoporev, *Int. J. Hydrog. Energy*, **46**, 32904 (2021)
2. Y.Y. Bozhko, R.K. Zhdanov, K.V. Gets, O.S. Subbotin, V.R. Belosludov, *J. Engin. Thermophys.* **32**, 62 (2023)
3. R.V. Belosludov, K.V. Gets, R.K. Zhdanov, Y.Y. Bozhko, V.R. Belosludov, Li-Jen Chen, Y. Kawazoe, *Molecules* **28** (7), 2960 (2023)
4. V.R. Belosludov, Y.Y. Bozhko, O.S. Subbotin, R.V. Belosludov, R.K. Zhdanov, K.V. Gets, Y. Kawazoe, *Molecules* **23**, 3336 (2018)
5. O.S. Subbotin Y.Y. Bozhko, R.K. Zhdanov, K.V. Gets, V.R. Belosludov, R.V. Belosludov, Y. Kawazoe, *Physical Chemistry Chemical Physics* **20**, 12637 (2018)
6. A.V. Meleshkin, N.V. Marasanov, *J. Engin. Thermophys.* **31**, 696 (2022)
7. A.V. Meleshkin, N.V. Marasanov, *J. Engin. Thermophys.* **30**, 699 (2021)
8. A.V. Meleshkin, A.A. Shkoldina, *J. Engin. Thermophys.* **30**, 693 (2021)
9. S. Misyura, P. Strizhak, A. Meleshkin, V. Morozov, O. Gaidukova, N. Shlegel, M. Shkola, *Energies* **16**, 3318 (2023)
10. J.Zheng, Z.R. Chong, M. F. Qureshi, P. Linga, *Energy Fuels* **34** (9), 10529 (2020)
11. P. Linga, R. Kumar, P. Englezos, *J. Hazard. Mater.* **149** (3), 625 (2007)
12. A.K. Sagidullin, A.S. Stoporev, A.Yu. Manakov, *Energy & Fuels* **33** (4), 3155 (2019)
13. S. Skiba, D. Strukov, A. Sagidullin, T. Adamova, A. Stoporev, L. Svarovskay, L. Strelets, L. Altunina and A. Manakov, *J. Pet. Sci. Eng.* **192**, 107211 (2020)
14. V.A. Shestakov, A.K. Sagidullin, A.S. Stoporev, *J. Mol. Liq.* **318**, 114018 (2020)
15. M.Y. Shumskayte, A.Yu. Manakov, A.K. Sagidullin, V.N. Glinskikh, L.S. Podenko, *Mar. Petrol. Geol.* **129**, 105096 (2021)
16. S.Y. Misyura, *Environ. Pollut.* **265**, 114871 (2020)
17. S.Y. Misyura, A.Y. Manakov, V.S. Morozov, G.S. Nyashina, O.S. Gaidukova, S.S. Skiba, R.S. Volkov, I.S. Voytkov, *J. Nat. Gas Sci. Eng.* **80**, 103396 (2020)
18. S.Y. Misyura, *Energy* **206**, 118120 (2020)
19. O.S. Gaydukova, S.Y. Misyura, P.A. Strizhak. *Combust. Flame* **228**, 78 (2021)
20. S.Y. Misyura, A.Y. Manakov, G.S. Nyashina, O.S. Gaidukova, V.S. Morozov, S.S. Skiba, *Entropy* **22**, 710 (2020)
21. S.Y. Misyura, I.G. Donskoy, A.Y. Manakov, V.S. Morozov, P.A. Strizhak, S.S. Skiba, A.K. Sagidullin, *J. Energy Storage* **44**, 103288 (2021)
22. A.V. Meleshkin, N.V. Marasanov, E.E. Schemeleva, *E3S Web of Conferences* **459**, 08004 (2023)